

MARViN - Multiple Arithmetic Resolutions Vacillating in Neural Networks

Lorenz Kummer¹² Kevin Sidak¹³ Tabea Reichmann¹⁴ Wilfried Gansterer¹⁵⁶

July 2021

Abstract

Quantization is a technique for reducing deep neural networks (DNNs) training and inference times, which is crucial for training in resource constrained environments or time critical inference applications. State-of-the-art (SOTA) quantization approaches focus on post-training quantization, i.e. quantization of pre-trained DNNs for speeding up inference. Very little work on quantized training exists, which neither allows dynamic intra-epoch precision switches nor employs an information theory based switching heuristic. Usually, existing approaches require full precision refinement afterwards and enforce a global word length across the whole DNN. This leads to suboptimal quantization mappings and resource usage. Recognizing these limits, we introduce MARViN, a new quantized training strategy using information theory-based intra-epoch precision switching, which decides on a *per-layer* basis which precision should be used in order to minimize quantization-induced information loss. Note that any quantization must leave enough precision such that future learning steps do not suffer from vanishing gradients. We achieve an average speedup of 1.86 compared to a float32 basis while limiting mean accuracy degradation on AlexNet/ResNet to only -0.075% .

1 Introduction

With the general trend in machine learning leaning towards large model sizes to solve increasingly complex problems, these models can be difficult to tackle in the context of inference in time critical applications or training under resource and/or productivity constraints. Some applications, where a more time- and space efficient model is crucial, include robotics, augmented reality, self driving vehicles, mobile applications, applications running on consumer hardware or research, needing a high number of trained models for hyper parameter optimization. Accompanied by this, DNN architectures, already some of the most common ones, like AlexNet or [1] ResNet [2], suffer from over-parameterization and overfitting.

Possible solutions to the aforementioned problems include pruning [3, 4, 5, 6, 7, 8], or quantization. When quantizing, the bitwidth of the parameters is decreased, therefore utilizing a lower precision for more efficient use of computing resources, such as memory and runtime. However, quantization has to be performed with a certain caution, as naive approaches or a too low bitwidth can have a negative impact on the accuracy of the network, unacceptable for most use cases. E.g. Binary Quantization [9] can effectively speed up computation, as multiplication can be performed as bit shifts, and further reduce memory, but the accuracy suffers heavily from this approach.

Prior approaches mainly quantize the network for inference, or use a global bitwidth, which does not take the differences quantization can have on different lay-

¹Faculty of Computer Science, University of Vienna

²lorenz.kummer@univie.ac.at

³kevin.sidak@univie.ac.at

⁴tabea.reichmann@univie.ac.at

⁵wilfried.gansterer@univie.ac.at

⁶PI

ers into account, nor use a dynamic precision switching mechanism based on information theory.

MARViN extends these approaches and introduces a new precision switching mechanism by applying the Kullback-Leibler-Divergence [10], that calculates the average number of bits lost due to a precision switch. This is done not only for the whole network, but on a per-layer basis, therefore considering differences of effect of quantization on the different layers. Further, our approach does not need full precision refinement, leading to an already quantized network that can then also be deployed on mobile hardware.

1.1 Related Work

In general studies of the sensitivity of DNNs, perturbation analysis [11] has been applied to examine historical neural network architectures [12, 13, 14] but also yielded results for the sensitivity of simple modern architectures recently [15].

For exploring the accuracy degradation induced by quantizations of weights, activations and gradients, [16] and [17] introduced the frameworks TensorQuant and QPyTorch, capable of simulating the most common quantizations for training and inference tasks on a float32 basis. Both frameworks allow to freely choose exponent and mantissa for floating-point, word and fractional bit length for fixed-point and word length for block-floating-point representations as well as signed/unsigned representations. Since the quantizations are simulations, no actual speedup can be achieved using these frameworks.

Minimizing inference accuracy degradation, induced by quantizing weights and activations, while leveraging associated performance increases can be achieved by incorporating (simulated) quantization into model training and training the model itself to compensate the introduced errors (Quantization Aware Training, QAT) [18, 19], by learning optimal quantization schemes through jointly training DNNs and associated quantizers (Learned Quantization Nets, LQ-Nets) [20] or by using dedicated quantization friendly operations [21]. A notably different

approach is taken by Variational Network Quantization (VNQ) [22] which uses variational Dropout training [23] with a structured sparsity inducing prior [24] to formulate post-training quantization as the variational inference problem searching the posterior optimizing the Kullback-Leibler-Divergence (KLD) [10].

For training on multi-node environments (i.e. distributed), Quantized Stochastic Gradient Descent (QSGD) introduced by [25] incorporates a family of gradient compression schemes aimed at reducing inter-node communication costs occurring during SGD’s gradient updates, producing a significant speedup as well as convergence guarantees under standard assumptions (not included here for brevity, see [26] for details). For speeding up training on a single node via block-floating point quantization, [27] introduced a dynamic training quantization scheme (Multi Precision Policy Enforced Training, MuPPET) that after quantized training outputs a model for float32 inference.

1.2 Contributions

We found the SOTA in quantized training and inference solutions leaves room for improvements in several areas. QAT, LQ-Nets and VNQ are capable of producing networks s.t. inference can be executed under quantization with minimal DNN degradation, but require computationally expensive float32 training. MuPPET requires at least N epochs for N quantization levels because precision switches are only triggered at the end of an epoch and going through all precision levels is required by the algorithm. Word length is global across the network such that potential advantages coming from different layers of the network storing different amounts of information are negated. The precision switching criterion is only based on the diversity of the gradients of the last k epochs, no metric is used to measure the actual amount of information lost by applying a certain quantization level to a weights tensor. Precision levels can only increase during training and never decrease. Furthermore, the network produced by MuPPET can only be used for float32

inference. We advance the SOTA by providing an easy-to-use solution for quantized training of DNNs by using an information-theoretical intra-epoch precision switching mechanism capable of dynamically increasing and decreasing the precision of the network on a per-layer basis, resulting in a network for inference that benefits in terms of runtime and model size from being quantized to the lowest precision possible for each layer. Besides its intrinsic methodological advantages, we demonstrate MARViN is competitive in accuracy degradation and superior in runtime, training AlexNet and ResNet20 on the CIFAR10/100 datasets.

2 Background

2.1 Quantization

Numerical representation describes how numbers are stored in memory (illustrated by fig. 1) and how arithmetic operations on those numbers are conducted. Commonly available on consumer hardware are floating-point and integer representations while fixed-point or block-floating-point representations are used in high-performance ASICs or FPGAs. The numerical precision used by a given numerical representation refers to the amounts of bits allocated for the representation of a single number, e.g. a real number stored in float32 refers to float-point representation in 32-bit precision. With these definitions of numerical representation and precision in mind, most generally speaking, quantization is the concept of running a computation or parts of a computation at reduced numerical precision or a different numerical representation with the intent of reducing computational costs and memory consumption. Quantized execution of a computation however can lead to the introduction of an error either through the quantized representations ϵ_{mach} being too large (underflow) to accurately depict resulting real values or the representable range being too small to store the result (overflow).

The value v of a floating point number is given by $v = \frac{s}{b^{p-1}} \times b^e$ where s is the significand (man-

tissa), p is the precision (number of digits in s), b is the base and e is the exponent [28]. Hence quantizing using floating-point representation can be achieved by reducing the number of bits available for mantissa and exponent, e.g. switching from a float32 to a float16 representation, and is offered out of the box by common machine learning frameworks for post-training quantization and quantized training [29, 30].

Integer representation is available for post-training quantization and QAT (int8, int16 due to availability on consumer hardware) in common machine learning frameworks [29, 30]. Quantized training however is not supported by these frameworks due to integer functions not being differentiable.

Block-floating-point represents each number as a pair of WL (word length) bit signed integer x and a scale factor s s.t. the value v is represented as $v = x \times b^{-s}$ with base $b = 2$ or $b = 10$. The scaling factor s is shared across multiple variables (blocks), hence the name block-floating point, and is typically determined s.t. the modulus of the largest element is $\in [\frac{1}{b}, 1]$ [31]. Block-Floating-Point arithmetic is used in cases where variables cannot be expressed with sufficient accuracy on native fixed-point hardware.

Fixed-point numbers have a fixed number of decimal digits assigned and hence every computation must be framed s.t. the results lies within the given boundaries of the representation [32]. By definition of [33], a signed fixed-point numbers of word length $WL = i + s + 1$ can be represented by a 3-tuple $\langle s, i, p \rangle$ where s denotes whether the number is signed, i denotes the number of integer bits and p denotes the number of fractional bits.

MARViN uses fixed-point quantization because unlike block floating point as used by MuPPET with a global word length across the whole network and per-layer shared exponent, we think that word length should be a local property of each layer under the hypothesis that different layers contain different amounts of information during different points of time in training. We decided against floating-point



Figure 1: Examples of floating-point, fixed-point and block-floating-point representations at different numerical precisions

quantization because fixed-point is available in high performance ASICS which is our target platform and against integer quantization due the fact that gradients cannot be computed for integer quantized networks.

2.2 MuPPET

MuPPET is a mixed-precision DNN training algorithm that combines the use of block-floating and floating-point representations. The algorithm stores two copies of the networks weights: a float32 master copy of the weights that is updated during backwards passes and a quantized copy used for forward passes. MuPPET uses block-floating point representation as outlined in sec. 2.1 for quantization. The precision level i of a layer l of all layers \mathbb{L} is defined as $q_l^i = \langle q_l^i | \forall l \in [1, |\mathbb{L}|] \rangle^i$:

$$q_l^i = \langle WL^{net}, s_l^{weights}, s_l^{act} \rangle^i \quad (1)$$

with WL being global across the network, and scaling factor s varying per layer, determined each time precision switch is triggered. The scaling factor for a

matrix X is given by

$s^{weights,act}$

$$= \left\lfloor \log_2 \min \left(\left(\frac{UB + 0.5}{\mathbf{X}_{max}^{weights,act}}, \frac{LB - 0.5}{\mathbf{X}_{min}^{weights,act}} \right) \right) \right\rfloor \quad (2)$$

with $\mathbf{X}_{max,min}^{weights,act}$ describing the maximum or minimum value in the weights or feature maps matrix of the layer. UB and LB describe the upper bounds and lower bounds of the word length WL^{net} . Its individual elements are quantized as described in eq. 3

$$x_{quant}^{\{weights,act\}} = \lfloor x^{\{weights,act\}} * 2^{s^{\{weights,act\}}} + Unif(-0.5, 0.5) \rfloor \quad (3)$$

$Unif(a, b)$ is the sampling from a uniform distribution in the interval $[a, b]$. The parameters 0.5 and -0.5 to add to the bounds is chosen for maximum utilisation of WL^{net} . During training the precision of the quantized weights is increased using a precision-switching heuristic based on gradient diversity [34], where the gradient of the last mini-batch $\nabla f_l^j(w)$ of each layer $l \in \mathbb{L}$ is stored and after a certain number of epochs (r), the inter-epoch gradient diversity at epoch j is computed by:

$$\Delta s(w)^j = \frac{\sum_{\forall l \in \mathbb{L}} \frac{\sum_{k=j-r}^j \|\nabla f_l^k(w)\|_2^2}{\|\sum_{k=j-r}^j \nabla f_l^k(w)\|_2^2}}{\mathbb{L}} \quad (4)$$

At epoch j there exists a set of gradient diversities $S(j) = \{\Delta s(w)^i | \forall e \leq i < j\}$ of which the ratio $p = \frac{\max S(j)}{\Delta s(w)^i}$ is calculated. If p violates a threshold for a certain number of times, a precision switch is triggered. Speedups claimed by MuPPET are based on an estimated performance model simulating fixed-point arithmetic using NVIDIA CUTLASS [35] for compatibility with GPUs, only supporting floating and integer arithmetic.

3 MARViN

3.1 Quantization Friendly Initialization

It has not yet been explored how quantized training impacts vanishing/exploding gradients, counter-strategies and vice versa. However the preliminary experimental results of our first investigation of the impact of different weights initialization strategies (Random Normal, Truncated Normal, Random Uniform, Glorot Normal/Uniform [36], He Normal/Uniform [37], Variance Scaling [38], Lecun Normal/Uniform [39, 40]) showed the resilience of DNNs trained under a fixed integer quantization scheme depends significantly on the initializer choice (fig. 2). We further found that DNNs initialized by fan-in truncated normal variance scaling (TNVS) degrade least under quantized training with a fixed integer quantization scheme. We thus initialize networks with TNVS and an empirically chosen scaling factor s , $\mu = 0$ and $\sigma = \sqrt{\frac{s}{n}}$ where n is the number of input units of a weights tensor before quantized training with MARViN. The examination of how other counter strategies (eg. gradient amplification, [43], gradient normalization [44], weights normalization [45]) affect quantized training remains an open question.

3.2 Precision Levels

MARViN uses signed fixed-point representation and stochastic rounding for quantizing float32 numbers. By definition of [33], a signed fixed-point number of world length WL is represented by a 3-tuple $\langle s, i, p \rangle$ where s denotes whether the number is signed, i denotes the number of integer bits and p denotes the number of fractional bits. Given that MARViN is agnostic towards whether a number is signed or not, we represent the precision level of each $l \in \mathbb{L}$ simply as $\langle WL^l, FL^l \rangle$ whereby fractional length FL^l denotes the number of fractional bits. For a random number $P \in [0, 1]$, x is stochastically rounded by

$$SR(x) = \begin{cases} \lfloor x \rfloor, & \text{if } P \geq \frac{x - \lfloor x \rfloor}{\epsilon} \\ \lfloor x \rfloor + 1, & \text{if } P < \frac{x - \lfloor x \rfloor}{\epsilon} \end{cases} \quad (5)$$

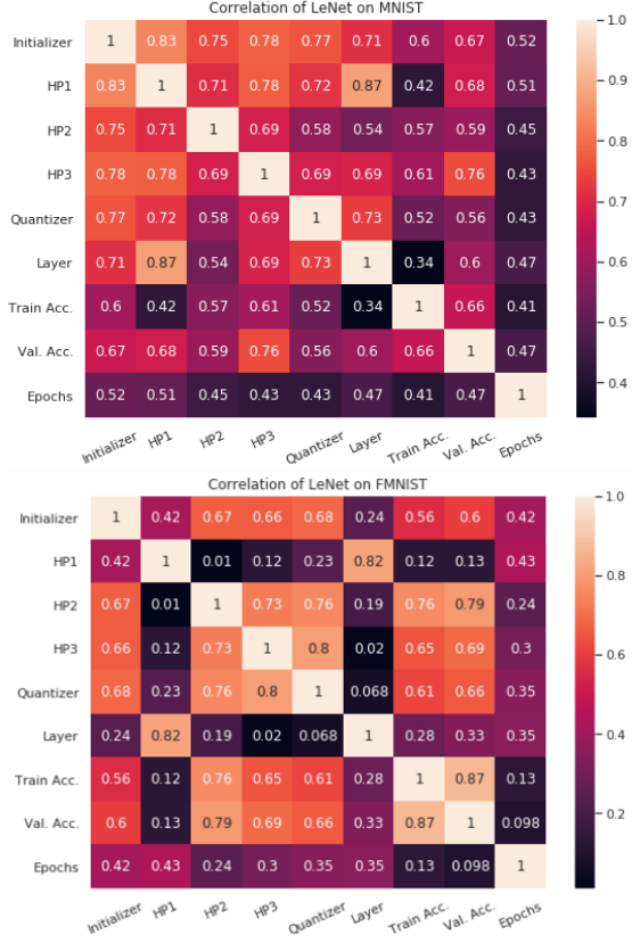


Figure 2: *Correlation of initializer choice, hyperparameters (HP), quantizer, layer, training and validation accuracy, duration of training (epochs) for LeNet5 [41] on MNIST and FMNIST datasets [42]*

3.3 Precision Switching Mechanism

Precision switching in quantized DNN training is the task of carefully balancing the need to keep precision as low as possible in order to improve runtime and model size, yet still keep enough precision for the network to keep learning. In MARViN, we have encoded these opposing interests in two operations, the PushDown Operation and the PushUp Operation.

The PushDown Operation Determining the amount of information lost if the precision of the fixed-point representation of a layer’s weight tensor is lowered, can be heuristically accomplished by interpreting the precision switch as a change of encoding. Assume a weights tensor $W^l \sim Q$ of layer $l \in \mathbb{L}$ with its quantized counterpart $\widehat{W}^l \sim P^l$, where P^l, Q^l are the respective distributions. Then the continuous Kullback-Leibler-Divergence [10] (6) represents the average number of bits lost through changing the encoding of l from Q^l to P^l .

$$D(P^l \| Q^l) = \int_{-\infty}^{\infty} p^l(w) \cdot \log \frac{p^l(w)}{q^l(w)} dw \quad (6)$$

Using discretization via binning, we obtain P^l and Q^l at resolution r^l through the empirical distribution function defined in eq. 7.

$$\widehat{F}_{r^l}(w) = \frac{1}{r^l + 1} \sum_{i=1}^{r^l} \mathbb{1}_{W_i^l \leq w} \quad (7)$$

that can then be used in the discrete Kullback-Leibler-Divergence (8).

$$KL(P^l \| Q^l) = \sum_{w \in W^l} P^l(w) \cdot \log \frac{P^l(w)}{Q^l(w)} \quad (8)$$

Using a bisection approach, MARViN efficiently finds the smallest quantization $\langle WL_{min}^l, FL_{min}^l \rangle$ of W^l s.t. $KL(P^l \| Q^l) > 0 \forall l \in \mathbb{L}$

The PushUp Operation However, determining the precision of the fixed-point representation of W^l at batch j , s.t. the information lost through quantization is minimal but there is still sufficient precision for subsequent batches $j + 1$ to keep learning, is a non-trivial task. Solely quantizing W^l at the beginning of the training to a low precision fix-point representation (e.g. $\langle WL^l, FL^l \rangle = \langle 8, 4 \rangle$) would result in the network failing to learn, because at such low precision levels, gradients would vanish very early on in the backwards pass. Hence, MARViN tracks for each layer a second heuristic over the last j batches to determine how much precision is required for the network to keep learning. If gradients are quantized,

a gradient diversity based heuristic is employed (9), (14).

$$\Delta s(w)_j^l = \frac{\sum_{k=j-r}^j \|\nabla f_k^l(w)\|_2}{\|\sum_{k=j-r}^j \nabla f_k^l(w)\|_2} \quad (9)$$

$$\Delta \tilde{s}(w)_j^l = \begin{cases} \log \Delta s(w)_j^l & \text{if } 0 < \Delta s(w)_j^l < \infty \\ 1 & \text{otherwise} \end{cases} \quad (10)$$

If $\Delta \tilde{s}(w)_j^l > 0$, two suggestions for an increase in precision are computed, $s_1^l = \max(\lceil \frac{1}{\log \Delta s(w)_j^l - 1} \rceil, 1)$ and $s_2^l = \max(\min(32 \cdot \log^2 \Delta s(w)_j^l - 1, 32) - FL_{min}^l, 1)$ and the final suggestion is computed dependent on a global strategy st via

$$s^l = \begin{cases} \min(s_1^l, s_2^l) & \text{if } st = \text{min} \\ \lceil 0.5 \cdot (s_1^l + s_2^l) \rceil & \text{if } st = \text{mean} \\ \max(s_1^l, s_2^l) & \text{if } st = \text{max} \end{cases} \quad (11)$$

Otherwise, i.e. $\Delta \tilde{s}(w)_j^l < 0$, $s^l = 1$. The new fixed-point quantization of layer l is then obtained by $WL^l = \min(\max(WL_{min}^l, FL_{min}^l) + 1, 32)$, $FL^l = (\min(FL_{min}^l + s^l, 32)$.

Strategy, Resolution and Lookback For adapting the strategy st mentioned in (11), we employ a simple loss-based heuristic. First we compute the average lookback over all layers $lb_{avg} = |\mathbb{L}|^{-1} \sum_{i=0}^{|\mathbb{L}|} lb^i$ and average loss $\mathcal{L}_{avg} = |\mathbb{L}|^{-1} \sum_{i=0}^{lb_{avg}} \mathcal{L}_i$ over the last lb_{avg} batches. Then via (12), the strategy is adapted.

$$st = \begin{cases} \max & \text{if } |\mathcal{L}_{avg}| \leq |\mathcal{L}_i| \text{ and } st = \text{'mean'} \\ \text{mean} & \text{if } |\mathcal{L}_{avg}| \leq |\mathcal{L}_i| \text{ and } st = \text{'min'} \\ \min & \text{if } |\mathcal{L}_{avg}| > |\mathcal{L}_i| \end{cases} \quad (12)$$

Because the number of gradients collected for each layer affects the result of the gradient diversity based heuristic (9), (14), we introduce a parameter lookback lb^l bounded by hyperparameters $lb_{lwr} \leq lb^l \leq lb_{upr}$ which is estimated at runtime. First, lb_{new} is computed (13), then, to prevent jitter,

a simple momentum is applied to obtain the updated $lb^l = [lb_{new}^l \cdot \gamma + (1 - \gamma) \cdot lb^l]$.

$$lb_{new}^l = \begin{cases} \min(\max(\lceil \frac{lb_{upr}}{\Delta s(w)_j^l} \rceil, lb_{lwr}), lb_{upr}) & \text{if } 0 < \Delta s(w)_j^l \\ lb_{upr} & \text{otherwise} \end{cases} \quad (13)$$

Similarly, the number of bins used in the discretization step (7) affects the result of the discrete Kullback-Leibler-Divergence (8). We control the number of bins via a parameter referred to as resolution r^l , which is derived at runtime and bounded by hyperparameters $r_{lwr} \leq r^l \leq r_{upr}$.

$$r^l = \begin{cases} \min(\max(r^l + 1, r_{lwr}), r_{upr}) & \text{if } lb^l = lb_{upr} \\ \min(\max(r^l - 1, r_{lwr}), r_{upr}) & \text{if } lb^l = lb_{lwr} \end{cases} \quad (14)$$

3.4 MARViN-SGD (MSGD)

Although MARViN can in principle be combined with any iterative gradient based optimizer (e.g. Adam [46]), we chose to implement MARViN with Stochastic Gradient Descent (SGD), because it generalizes better than adaptive gradient algorithms [47]. The implementation of MARViN employs the precision switching mechanism and numeric representation described in sec. 3, by splitting it in two operations: the PushDown Operation (alg. 3), which, for a given layer, finds the smallest fixed-point representation that causes no information loss, and the PushUp Operation (alg. 4), which, for a given layer, seeks the precision that is required for the network to keep learning. The integration of these two operations into the precision switching mechanism is depicted in alg. 2, and the integration into SGD training process is depicted in alg. 1. In addition to the MARViN precision switching mechanism, we used an L1 sparsifying regularizer [48, 49, 50] to obtain particularly quantization-friendly weight tensors, combined linearly with L2 regularization for better accuracy in a similar way as proposed by [51] (15).

$$\hat{\mathcal{L}}(W) = \alpha \|W\|_1 + \frac{\beta}{2} \|W\|_2^2 + \mathcal{L} \quad (15)$$

When MARViN-SGD (alg. 1) is started on untrained

Data: Untrained Float32 DNN
Result: Trained and Quantized DNN

```

1  $\hat{\mathbb{L}} = \text{InitFixedPointTNVS}()$ 
2  $\mathbb{Q} = \text{InitQuantizationMapping}(\hat{\mathbb{L}})$ 
3  $\mathbb{L} = \text{Float32Copy}(\hat{\mathbb{L}})$ 
4 for Epoch in Epochs do
5   for Batch in Batches do
6      $\hat{\mathbb{G}}, \mathcal{L} = \text{ForwardPass}(\hat{\mathbb{L}}, \text{Batch})$ 
7      $\mathbb{Q} = \text{PrecisionSwitch}(\hat{\mathbb{G}}, \mathcal{L}, \mathbb{Q}, \mathbb{L})$ 
8      $\text{SGDBackwardsPass}(\mathbb{L}, \hat{\mathbb{G}})$ 
9     for  $l \in \mathbb{L}$  do
10       $\hat{\mathbb{L}}[l] = \text{Quantize}(\mathbb{L}[l], \mathbb{Q}[l][\text{quant}])$ 
11   end
12 end
13 end
```

Algorithm 1: MARViN-SGD

float32 DNN, it first initializes the DNNs' weights (denoted as $\hat{\mathbb{L}}$) with TNVS (alg. 1, ln. 1). Next the quantization mapping \mathbb{Q} is initialized, which assigns each $l \in \mathbb{L}$ a tuple $\langle WL^l, FL^l \rangle$, a lookback lb^l and a resolution r^l (alg. 1, ln. 2). Then a float32 master copy \mathbb{L} of $\hat{\mathbb{L}}$ is created (alg. 1, ln. 3). During training for each forward pass on a batch of data, quantized gradients $\hat{\mathbb{G}}$ and loss \mathcal{L} are computed with a forward pass using quantized layers $\hat{\mathbb{L}}$ (alg. 1, ln. 4-6). The precision switching mechanism described in sec. 3 is then called (alg. 1, ln. 7) and after adapting the push up strategy as described in sec. 3, it iterates over $l \in \mathbb{L}$ (alg. 2 ln. 2), first adapting resolution r^l and lookback lb^l (alg. 2 ln. 4-5) and then executing PushDown and PushUp on layer l (alg. 2 ln. 6 -10) to update $\langle WL^l, FL^l \rangle \in \mathbb{Q}$. When PushDown is called on l , it decreases the quantization mapping in a bisectional fashion until KL indicates a lower quantization would cause information loss at resolution r^l (3, ln. 1-5). After computing the lowest quantization $\langle WL_{min}^l, FL_{min}^l \rangle \in \mathbb{Q}$ not causing information loss in l , PushUp is called on l to increase the quantization to the point where the network is expected to keep learning, based on gradient diversity of the last lb^l batches (alg. 4, ln. 1-6). After PushUp the PrecisionSwitch returns an updated \mathbb{Q} to the training

```

Data:  $\widehat{\mathbb{G}}, \mathcal{L}, \mathbb{Q}, \mathbb{L}$ 
Result:  $\mathbb{Q}$ 
1 AdaptStrategy( $\mathcal{L}$ )
2 for  $l \in \mathbb{L}$  do
3    $\mathbb{Q}[l][grads].append(\widehat{\mathbb{G}}[l])$ 
4   AdaptLookback( $\mathbb{Q}[l][grads], \mathbb{Q}[l][lb]$ )
5   AdaptResolution( $\mathbb{Q}[l][lb], \mathbb{Q}[l][res]$ )
6   if  $|\mathbb{Q}[l][grads]| \geq \mathbb{Q}[l][lb]$  then
7      $WL^l, FL^l = \mathbb{Q}[l][quant]$ 
8      $WL_{min}^l, FL_{min}^l = \text{PushDown}(\mathbb{L}[l],$ 
       $WL^l, FL^l)$ 
9      $WL_{new}^l, FL_{new}^l = \text{PushUp}(l, WL^l,$ 
       $FL^l, WL_{min}^l, FL_{min}^l)$ 
10     $\mathbb{Q}[l][quant] = WL_{new}^l, FL_{new}^l$ 
11  end
12 end

```

Algorithm 2: PrecisionSwitch

```

Data:  $L, WL^l, FL^l$ 
Result:  $WL_{min}^l, FL_{min}^l$ 
1  $WL_{min}^l, FL_{min}^l = L, WL^l, FL^l$ 
2 repeat
3    $WL_{min}^l, FL_{min}^l = \text{Decrease}(WL_{min}^l,$ 
     $FL_{min}^l)$ 
4    $\widehat{L} = \text{Quantize}(L, WL_{min}^l, FL_{min}^l)$ 
5 until  $KL(EDF(L_i), EDF(\widehat{L})) < \epsilon$ 

```

Algorithm 3: PushDown Operation

```

Data:  $L, WL^l, FL^l, WL_{min}^l, FL_{min}^l$ 
Result:  $WL_{new}^l, FL_{new}^l$ 
1 Compute  $\widehat{\Delta s(L)}$  using  $WL_{min}^l, WL_{min}^l$ 
2 Compute  $\Delta s(L)$  using  $WL^l, FL^l$ 
3 while  $\Delta s(L) \geq \widehat{\Delta s(L)}$  do
4    $WL_{min}^l, FL_{min}^l = \text{Increase}(WL_{min}^l,$ 
     $FL_{min}^l)$ 
5   Compute  $\widehat{\Delta s(L)}$  using  $WL_{min}^l, FL_{min}^l$ 
6 end

```

Algorithm 4: PushUp Operation

loop, and a regular SGD backward pass updates the float32 master copy \mathbb{L} , using quantized gradients $\widehat{\mathbb{G}}$ (alg. 1, ln. 7,8). Finally, the now updated weights \mathbb{L} are quantized using the updated \mathbb{Q} and written back to $\widehat{\mathbb{L}}$ to be using in the next forward pass (alg. 1, ln. 9-11).

4 Experimental Evaluation

4.1 Setup

For experimental evaluation of MARViN, we trained AlexNet [1] and ResNet20 [52] on the CIFAR-10/100 [53] datasets. Due to unavailability of fixed-point hardware, we used QPyTorch [17] to simulate fixed point arithmetic on our faculties DGX-1 cluster, with 8 x Tesla V100 GPUs, which is only capable of integer and floating-point arithmetic [54]. Speedups and model size reductions were computed using a performance model taking forward and backward passes, as well as batch sizes, into account. The performance model computes per layer MADDs, weights them with the layer’s world length at a specific stage in training, and aggregates them to obtain the overall incurred computational costs. All layers were quantized with $\langle WL, FL \rangle = \langle 8, 4 \rangle$ at the beginning of MARViN training, other hyperparameters were selected using 10-fold cross-validation.

4.2 Results

Tab. 1 shows the top-1 validation accuracies and accuracy differences achieved by MARViN (*) and MuPPET (‘) for both quantized training on CIFAR100, and a float32 basis. Tab. 2 shows results for training on CIFAR10. As can be seen in the tables, MARViN is capable of quantized training to an accuracy comparable to float32 training, and in 50% of the examined cases even surpassed the baseline accuracy. MARViN does so while requiring on average 25% less epochs compared to MuPPET. The chosen experiments furthermore illustrate that MARViN delivers this performance independent of the underlying DNN architecture or the dataset used. Fig. 3 and 4 display word length usage over time for individual

	CIFAR100		
	Float32	Quantized	Δ
AlexNet*	44.2 ¹⁰⁰ ₂₅₆	45.0 ¹⁰⁰ ₂₅₆	0.1
AlexNet'	38.2 ¹⁵⁰ ₁₂₈	38.2 ¹⁵⁰ ₁₂₈	0.0
ResNet20*	65.7 ¹⁰⁰ ₂₅₆	65.4 ¹⁰⁰ ₂₅₆	-0.3
ResNet20'	64.6 ¹⁵⁰ ₁₂₈	65.8 ¹⁵⁰ ₁₂₈	1.2

Table 1: Top-1 accuracies, MARViN (ours, marked with *) vs MuPPET (marked with '), CIFAR10, 100 to 150 epochs. Float 32 indicates 32-bit floating-point training (baseline), Quantized indicates variable bit fix-point (MARViN) or block-floating-point (MuPPET) quantized training, subscript indicates batch size used, superscript indicates epochs used

	CIFAR10		
	Float32	Quantized	Δ
AlexNet*	77.1 ¹⁵⁰ ₂₅₆	75.8 ^{150*} ₂₅₆	-1.4
AlexNet'	75.5 ¹⁵⁰ ₁₂₈	74.5 ¹⁵⁰ ₁₂₈	-1.0
ResNet20*	89.0 ^{100*} ₂₅₆	90.4 ¹⁰⁰ ₂₅₆	1.3
ResNet20'	90.1 ¹⁵⁰ ₁₂₈	90.9 ¹⁵⁰ ₁₂₈	0.8

Table 2: Top-1 accuracies, MARViN (ours, *) vs MuPPET (marked with '), CIFAR100

	CIFAR10			
	MEM	SZ	SU*	SU'
AlexNet*	0.69	0.73	1.2	1.73
AlexNet'	0.66	1.0	-	1.33
ResNet20*	0.70	0.72	1.32	1.86
ResNet20'	0.61	1.0	-	1.38

Table 4: Memory Footprint, Final Model Size, Memory Footprint, Speedup, MARViN (ours, *) vs MuPPET (marked with ') on respective baseline float32 training on CIFAR10

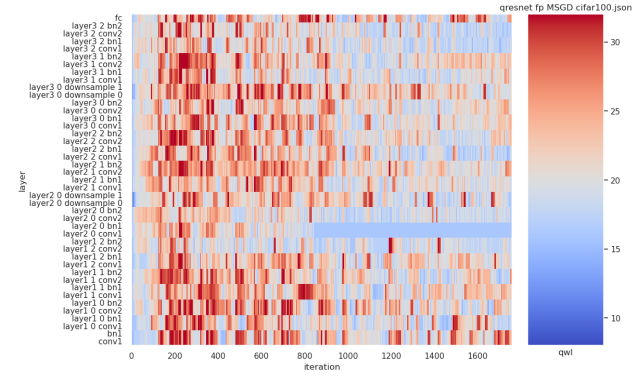


Figure 3: Wordlengths (bit) of MSGD optimized ResNet20 on CIFAR100

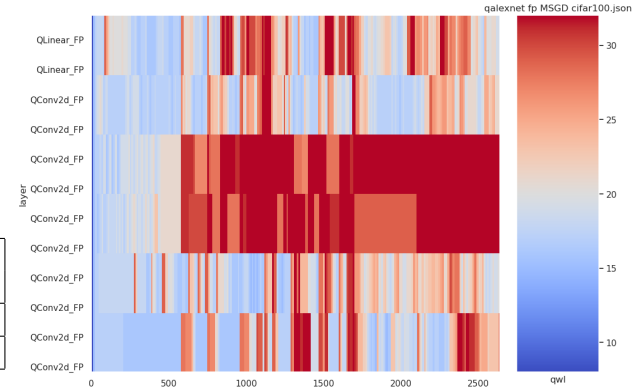


Figure 4: Wordlengths (bit) of MSGD optimized AlexNet on CIFAR10

layers for ResNet20 and AlexNet on CIFAR100. In both cases, we observe that individual layers have different precision preferences dependent on progression of the training, an effect that is particularly pronounced in AlexNet. For ResNet20, the word length interestingly decreased in the second half of training, which we conjecture is attributable to sparsifying L1 regularization leading to a reduction in irrelevant weights, that would otherwise offset the KL heuristic used in the PushDown Operation. Tabs. 3 and 4

	CIFAR100			
	MEM	SZ	SU*	SU'
AlexNet*	0.51	0.44	1.46	1.99
ResNet20*	0.68	0.64	1.31	1.85

Table 3: Memory Footprint, Final Model Size, Speedup, MARViN (ours, *) vs MuPPET (marked with ') on respective baseline float32 training on CIFAR100

show MARViNs estimated speedups vs. our float32 baseline (100 epochs, same number of gradient accumulation steps and batch size as MARViN trained models) and MuPPETs float32 baseline. MARViN training achieves speedups comparable with SOTA solutions on our own baseline and outperforms MuPPET on MuPPETs baseline in every evaluated scenario. Unfortunately, the code provided by MuPPET could not be executed so we were unable to apply MuPPET to the more efficient MARViN baseline.

5 Conclusion

With MARViN we introduce a novel mixed-precision DNN training algorithm that can be combined with any iterative gradient based training scheme. MARViN exploits fast fixed-point operations for forward passes, while executing backward passes in highly precise float32. By carefully balancing the need to minimize the fixed-point precision for maximum speedup and minimal memory requirements, while at the same time keeping precision high enough for the network to keep learning, our approach produces top-1 accuracies comparable or better than SOTA float32 techniques or other quantized training algorithms. Furthermore MARViN has the intrinsic methodical advantage of not only training the network in a quantized fashion, but also the trained network itself is quantized s.t. it can be deployed to fast ASIC hardware.

6 Future Work

MARViN as presented employs a fixed-point representation to enable fine granular precision switches. However, fixed-point hardware is not as common as floating-point hardware, so we plan to extend the concept to floating point quantization s.t. MARViN becomes compatible with float16/float32 consumer hardware. Additionally, we conjecture the heuristics used by MARViN can be used for intra-training DNN pruning as well, which will be subject to future research.

References

- [1] A. Krizhevsky, I. Sutskever, and G. E. Hinton, “Imagenet classification with deep convolutional neural networks,” in *Advances in neural information processing systems*, pp. 1097–1105, 2012.
- [2] K. He, X. Zhang, S. Ren, and J. Sun, “Deep residual learning for image recognition,” in *Proceedings of the IEEE conference on computer vision and pattern recognition*, pp. 770–778, 2016.
- [3] A. Gordon, E. Eban, O. Nachum, B. Chen, H. Wu, T.-J. Yang, and E. Choi, “Morphnet: Fast & simple resource-constrained structure learning of deep networks,” in *Proceedings of the IEEE conference on computer vision and pattern recognition*, pp. 1586–1595, 2018.
- [4] F. N. Iandola, S. Han, M. W. Moskewicz, K. Ashraf, W. J. Dally, and K. Keutzer, “SqueezeNet: Alexnet-level accuracy with 50x fewer parameters and 0.5 mb model size,” *arXiv preprint arXiv:1602.07360*, 2016.
- [5] S. Han, H. Mao, and W. J. Dally, “Deep compression: Compressing deep neural network with pruning, trained quantization and huffman coding,” in *4th International Conference on Learning Representations, ICLR 2016, San Juan, Puerto Rico, May 2-4, 2016, Conference Track Proceedings* (Y. Bengio and Y. LeCun, eds.), 2016.
- [6] J. Fang, Y. Sun, Q. Zhang, K. Peng, Y. Li, W. Liu, and X. Wang, “Fna++: Fast network adaptation via parameter remapping and architecture search,” *IEEE Transactions on Pattern Analysis and Machine Intelligence*, pp. 1–1, 2020.
- [7] W. Hua, Y. Zhou, C. M. De Sa, Z. Zhang, and G. E. Suh, “Channel gating neural networks,” in *Advances in Neural Information Processing Systems* (H. Wallach, H. Larochelle, A. Beygelzimer, F. d’Alché-Buc, E. Fox, and R. Garnett, eds.), vol. 32, Curran Associates, Inc., 2019.

[8] M. Lis, M. Golub, and G. Lemieux, “Full deep neural network training on a pruned weight budget,” in *Proceedings of Machine Learning and Systems* (A. Talwalkar, V. Smith, and M. Zdziarska, eds.), vol. 1, pp. 252–263, 2019.

[9] M. Courbariaux, I. Hubara, D. Soudry, R. El-Yaniv, and Y. Bengio, “Binarized neural networks: Training deep neural networks with weights and activations constrained to +1 or -1,” 02 2016.

[10] S. Kullback and R. A. Leibler, “On information and sufficiency,” *The annals of mathematical statistics*, vol. 22, no. 1, pp. 79–86, 1951.

[11] N. J. Higham, *Accuracy and Stability of Numerical Algorithms*, ch. 7, pp. 119–137.

[12] K. Wang and A. N. Michel, “Robustness and perturbation analysis of a class of artificial neural networks,” *Neural Networks*, vol. 7, no. 2, pp. 251–259, 1994.

[13] A. Meyer-Base, “Perturbation analysis of a class of neural networks,” in *Proceedings of International Conference on Neural Networks (ICNN’97)*, vol. 2, pp. 825–828 vol.2, 1997.

[14] Xiaoqin Zeng and D. S. Yeung, “Sensitivity analysis of multilayer perceptron to input and weight perturbations,” *IEEE Transactions on Neural Networks*, vol. 12, no. 6, pp. 1358–1366, 2001.

[15] L. Xiang, X. Zeng, Y. Niu, and Y. Liu, “Study of sensitivity to weight perturbation for convolution neural network,” *IEEE Access*, vol. 7, pp. 93898–93908, 2019.

[16] D. M. Loroch, F.-J. Pfreundt, N. Wehn, and J. Keuper, “Tensorquant: A simulation toolbox for deep neural network quantization,” in *Proceedings of the Machine Learning on HPC Environments*, pp. 1–8, 2017.

[17] T. Zhang, Z. Lin, G. Yang, and C. De Sa, “Qpytorch: A low-precision arithmetic simulation framework,” *arXiv preprint arXiv:1910.04540*, 2019. <https://arxiv.org/pdf/1910.04540.pdf>

[18] B. Jacob, S. Kligys, B. Chen, M. Zhu, M. Tang, A. Howard, H. Adam, and D. Kalenichenko, “Quantization and training of neural networks for efficient integer-arithmetic-only inference,” in *Proceedings of the IEEE Conference on Computer Vision and Pattern Recognition*, pp. 2704–2713, 2018.

[19] J. Yang, X. Shen, J. Xing, X. Tian, H. Li, B. Deng, J. Huang, and X.-s. Hua, “Quantization networks,” in *Proceedings of the IEEE Conference on Computer Vision and Pattern Recognition*, pp. 7308–7316, 2019.

[20] D. Zhang, J. Yang, D. Ye, and G. Hua, “Lq-nets: Learned quantization for highly accurate and compact deep neural networks,” in *Proceedings of the European Conference on Computer Vision (ECCV)*, September 2018.

[21] T. Sheng, C. Feng, S. Zhuo, X. Zhang, L. Shen, and M. Aleksic, “A quantization-friendly separable convolution for mobilenets,” in *2018 1st Workshop on Energy Efficient Machine Learning and Cognitive Computing for Embedded Applications (EMC2)*, pp. 14–18, IEEE, 2018.

[22] J. Achterhold, J. M. Koehler, A. Schmeink, and T. Genewein, “Variational network quantization,” in *International Conference on Learning Representations*, 2018.

[23] D. P. Kingma, T. Salimans, and M. Welling, “Variational dropout and the local reparameterization trick,” *arXiv preprint arXiv:1506.02557*, 2015. <https://arxiv.org/pdf/1506.02557.pdf>

[24] K. Neklyudov, D. Molchanov, A. Ashukha, and D. Vetrov, “Structured bayesian pruning via log-normal multiplicative noise,” *arXiv preprint arXiv:1705.07283*, 2017. <https://arxiv.org/pdf/1705.07283.pdf>

[25] D. Alistarh, D. Grubic, J. Li, R. Tomioka, and M. Vojnovic, “Qsgd: Communication-efficient sgd via gradient quantization and encoding,” *Advances in Neural Information Processing Systems*, vol. 30, pp. 1709–1720, 2017.

[26] D. Alistarh, D. Grubic, J. Li, R. Tomioka, and M. Vojnovic, “Qsgd: Communication-efficient sgd via gradient quantization and encoding,” *arXiv preprint arXiv:1610.02132*, 2016. <https://arxiv.org/pdf/1610.02132.pdf>.

[27] A. Rajagopal, D. A. Vink, S. I. Venieris, and C.-S. Bouganis, “Multi-precision policy enforced training (muppet): A precision-switching strategy for quantised fixed-point training of cnns,” *arXiv preprint arXiv:2006.09049*, 2020.

[28] J. H. Wilkinson, *Rounding errors in algebraic processes*. Courier Corporation, 1994.

[29] A. Paszke, S. Gross, F. Massa, A. Lerer, J. Bradbury, G. Chanan, T. Killeen, Z. Lin, N. Gimelshein, L. Antiga, A. Desmaison, A. Kopf, E. Yang, Z. DeVito, M. Raison, A. Tejani, S. Chilamkurthy, B. Steiner, L. Fang, J. Bai, and S. Chintala, “Pytorch: An imperative style, high-performance deep learning library,” in *Advances in Neural Information Processing Systems 32* (H. Wallach, H. Larochelle, A. Beygelzimer, F. d’Alché-Buc, E. Fox, and R. Garnett, eds.), pp. 8024–8035, Curran Associates, Inc., 2019.

[30] M. Abadi, A. Agarwal, P. Barham, E. Brevdo, Z. Chen, C. Citro, G. S. Corrado, A. Davis, J. Dean, M. Devin, S. Ghemawat, I. Goodfellow, A. Harp, G. Irving, M. Isard, Y. Jia, R. Jozefowicz, L. Kaiser, M. Kudlur, J. Levenberg, D. Mané, R. Monga, S. Moore, D. Murray, C. Olah, M. Schuster, J. Shlens, B. Steiner, I. Sutskever, K. Talwar, P. Tucker, V. Vanhoucke, V. Vasudevan, F. Viégas, O. Vinyals, P. Warden, M. Wattenberg, M. Wicke, Y. Yu, and X. Zheng, “TensorFlow: Large-scale machine learning on heterogeneous systems,” 2015. Software available from tensorflow.org.

[31] J. H. Wilkinson, *Rounding errors in algebraic processes*. Courier Corporation, 1994.

[32] J. H. Wilkinson, *Rounding errors in algebraic processes*. Courier Corporation, 1994.

[33] M. Hopkins, M. Mikaitis, D. R. Lester, and S. Furber, “Stochastic rounding and reduced-precision fixed-point arithmetic for solving neural ordinary differential equations,” *Philosophical Transactions of the Royal Society A*, vol. 378, no. 2166, p. 20190052, 2020.

[34] D. Yin, A. Pananjady, M. Lam, D. Papailiopoulos, K. Ramchandran, and P. Bartlett, “Gradient diversity: a key ingredient for scalable distributed learning,” in *International Conference on Artificial Intelligence and Statistics*, pp. 1998–2007, 2018.

[35] A. Kerr, H. Wu, M. Gupta, D. Blasig, P. Ramanan, N. Farooqui, P. Majcher, P. Springer, J. Wang, S. Yokim, M. Hohnerbach, A. Atluri, D. Tanner, T. Costa, J. Demouth, B. Fahs, M. Goldfarb, M. Hagog, F. Hu, A. Kaatz, T. Li, T. Liu, D. Merrill, K. Siu, M. Tavennarath, J. Tran, V. Wang, J. Wu, F. Xie, A. Xu, J. Yang, X. Zhang, N. Zhao, G. Bharambe, C. Cecka, L. Durant, O. Giroux, S. Jones, R. Kulkarni, B. Lelbach, J. McCormack, and K. P. and, “Nvidia cutlass,” 2020. Online, accessed 15.07.2020.

[36] X. Glorot and Y. Bengio, “Understanding the difficulty of training deep feedforward neural networks,” in *Proceedings of the thirteenth international conference on artificial intelligence and statistics*, pp. 249–256, 2010.

[37] K. He, X. Zhang, S. Ren, and J. Sun, “Delving deep into rectifiers: Surpassing human-level performance on imagenet classification,” in *Proceedings of the IEEE international conference on computer vision*, pp. 1026–1034, 2015.

[38] B. Hanin and D. Rolnick, “How to start training: The effect of initialization and architecture,” in *Advances in Neural Information Processing Systems*, pp. 571–581, 2018.

[39] G. Klambauer, T. Unterthiner, A. Mayr, and S. Hochreiter, “Self-normalizing neural networks,” in *Advances in neural information processing systems*, pp. 971–980, 2017.

[40] Y. A. LeCun, L. Bottou, G. B. Orr, and K.-R. Müller, “Efficient backprop,” in *Neural networks: Tricks of the trade*, pp. 9–48, Springer, 2012.

[41] Y. LeCun, L. Bottou, Y. Bengio, and P. Haffner, “Gradient-based learning applied to document recognition,” *Proceedings of the IEEE*, vol. 86, no. 11, pp. 2278–2324, 1998.

[42] L. Deng, “The mnist database of handwritten digit images for machine learning research [best of the web],” *IEEE Signal Processing Magazine*, vol. 29, no. 6, pp. 141–142, 2012.

[43] S. Basodi, C. Ji, H. Zhang, and Y. Pan, “Gradient amplification: An efficient way to train deep neural networks,” *arXiv preprint arXiv:2006.10560*, 2020. <https://arxiv.org/pdf/2006.10560.pdf>

[44] Z. Chen, V. Badrinarayanan, C.-Y. Lee, and A. Rabinovich, “Gradnorm: Gradient normalization for adaptive loss balancing in deep multitask networks,” in *International Conference on Machine Learning*, pp. 794–803, 2018.

[45] T. Salimans and D. P. Kingma, “Weight normalization: A simple reparameterization to accelerate training of deep neural networks,” in *Advances in neural information processing systems*, pp. 901–909, 2016.

[46] D. P. Kingma and J. Ba, “Adam: A method for stochastic optimization,” *arXiv preprint arXiv:1412.6980*, 2014.

[47] P. Zhou, J. Feng, C. Ma, C. Xiong, S. C. H. Hoi, and W. E, “Towards theoretically understanding why sgd generalizes better than adam in deep learning,” in *Advances in Neural Information Processing Systems* (H. Larochelle, M. Ranzato, R. Hadsell, M. F. Balcan, and H. Lin, eds.), vol. 33, pp. 21285–21296, Curran Associates, Inc., 2020.

[48] P. M. Williams, “Bayesian regularization and pruning using a laplace prior,” *Neural computation*, vol. 7, no. 1, pp. 117–143, 1995.

[49] A. Y. Ng, “Feature selection, l 1 vs. l 2 regularization, and rotational invariance,” in *Proceedings of the twenty-first international conference on Machine learning*, p. 78, 2004.

[50] R. Tibshirani, “Regression shrinkage and selection via the lasso,” *Journal of the Royal Statistical Society: Series B (Methodological)*, vol. 58, no. 1, pp. 267–288, 1996.

[51] H. Zou and T. Hastie, “Regularization and variable selection via the elastic net,” *Journal of the royal statistical society: series B (statistical methodology)*, vol. 67, no. 2, pp. 301–320, 2005.

[52] K. He, X. Zhang, S. Ren, and J. Sun, “Deep residual learning for image recognition,” in *Proceedings of the IEEE conference on computer vision and pattern recognition*, pp. 770–778, 2016.

[53] G. H. Alex Krizhevsky, Vinod Nair, “The cifar-10 and cifar-100 dataset,” 2019. Online, accessed 15.07.2020.

[54] N. Corporation, “NVIDIA DGX-1essential instrument for ai research,” 2017. Online, accessed 07.07.2021.